Numerical simulation of heat transfer process in longitudinal section of a plate heat exchanger

Cite as: AIP Conference Proceedings **2486**, 020021 (2022); https://doi.org/10.1063/5.0105573
Published Online: 15 November 2022

Y. V. Vankov, E. V. Izmaylova, E. V. Garnyshova, et al.

Numerical Simulation of Heat Transfer Process in Longitudinal Section of a Plate Heat Exchanger

Y. V. Vankov[1], E. V. Izmaylova[1, a)], E. V. Garnyshova[1], A. M. Khvorystkina[1] and I. V. Shvetsov[2, b)]

[1] *Kazan State Power Engineering University, Kazan, Russia*
[2] *Yaroslav-the-Wise Novgorod State University, Veliky Novgorod, Russia*

[a)] Corresponding author: evgeniya-izmailova@yandex.ru
[b)] Igor.Shvetsov@novsu.ru

Abstract. The task of increasing energy efficiency in the production, transmission and use of thermal energy is relevant and directly depends on the efficiency of the used heat exchangers. In this work, a numerical simulation of the heat transfer process in a plate heat exchanger in a longitudinal section was carried out using the ANSYS software package. Four options of plates were considered: those with a sinusoidal, triangular, trapezoidal, and ellipsoidal profile. Based on the obtained simulation results, it was concluded that when considering the longitudinal section with increasing velocity, the shape of the corrugated plate affects the heat transfer characteristics to a lesser extent, and the hydraulic losses to a more extent. Based on the data, the curvature of the plates was modified to better match the flow style of hot and cold media.

INTRODUCTION

Heat exchange processes are widely used not only the in energy industry, but also in the chemical, food, metallurgical, oil refining industries, as well as in the municipal economy. Heat exchangers of various types use heating for cold media and cooling for hot media, processes of melting, crystallization, evaporation, condensation [1-3]. Therefore, the problem to improve energy efficiency in production, transfer and use of thermal energy is relevant and directly depends on the efficiency of heat exchangers applied.

Plate heat exchangers belonging to the class of recuperative heat exchangers are apparatus with the heat exchange surface formed by a set of thin stamped metal plates with a corrugated surface. Plates assembled in a single package form channels among themselves, through which heat carriers flow, exchanging thermal energy. Channels with heat carriers alternate.

Main dimensions and parameters of the plate heat exchangers most currently used in industry are defined in [4]. They are made with a heat exchange surface from 2 to 600 m^2 depending on the type and dimensions of plates; these heat exchangers are used at pressures up to 1.6 mPa and temperatures of operating media from от –30 to +180 °C to implement heat exchange between fluids and vapors (gases) as refrigerators, heaters and condensers.

The corrugations of the plates usually have an equilateral triangle profile in cross section. Plate material is galvanized or corrosion-resistant steel, titanium, aluminum.

Heat transfer depends on the plate profile. Various profiles of plates determined the coefficient of heat transfer. All plates in the package are similar, but are turned 180 degrees relative to each other, such an installation of the plates provides the alternation of hot and cold channels. This principle of constructing a heat exchanger makes it

IV International Scientific and Practical Conference on Innovations in Engineering and Technology (ISPCIET 2021)
AIP Conf. Proc. 2486, 020021-1–020021-9; https://doi.org/10.1063/5.0105573
Published by AIP Publishing. 978-0-7354-4269-6/$30.00

possible to quickly modify it, increasing the amount of plates and, consequently, the power of the heat exchanger, or repairing it easily in case of a failure of a rubber gasket or a heat exchange plate.

The design of apparatus allows assembling any (from 5 to 1750 m^2) heat exchange surface. The type and number of plates depends on the required heat transfer. The assembly of plates ensures reliable mutual sealing of flow channels, as well as determines the flow direction in the heat exchanger. Main technical data of heat exchangers (depending on the version) are presented in table 1.

TABLE 1. Main technical data of a heat exchange apparatus

Power	1 kW – 40 MW
Consumption	5 m^3– 4500 m^3
Plate area	0.04 m^2– 3.0 m^2
Connection diameter	DN25 – DN500
Working temperature	– 20°C-+195°C
Working pressure	max. 25 bar

By means of stamping, the heat exchanger plate is given a corrugated shape, which enhances the turbulence of the flows of working media, increasing the heat transfer coefficient and reducing the amount of salt and contamination deposits on the working surfaces of the plates. The plates are also subjected to electrochemical polishing, leading to a decrease in the hydraulic resistance of the slotted channel between the plates.

DESCRIPTION OF SAMPLES UNDER RESEARCH AND CONSTRUCTION OF CALCULATION MODELS

Consider the plate surface of a plate heat exchange apparatus (Fig. 1). Working part of its surface washed by a heat exchange flow inside the channel consists of a main corrugated field and zones of flow distribution at the inlet and outlet. Most of the heat is transferred to the main corrugated field, area of which reaches 80–85% of the total plate area. The distribution zones are subject to a significantly less heat exchange, but their impact on the total hydraulic resistance of the channel is great. In these zones the flow rates increase from the speed at the main working field to the speed at the outlet of the channel to the collection header (the same for the outlet from the distribution header).

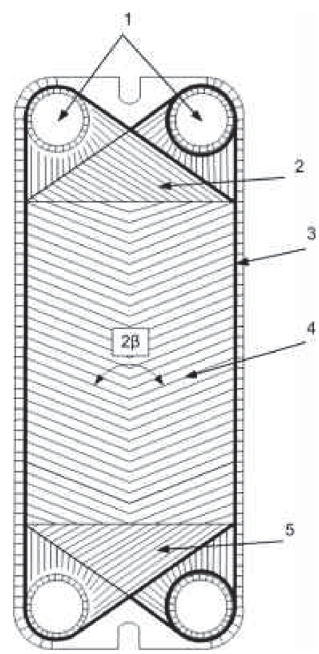

FIGURE 1. Schematic drawing of heat exchanger plate: 1 – inlet and outlet of heat carrier; 2, 5 – flow distribution zones; 3 – rubber gasket; 4 – the main corrugated field

The design of the corrugations in the distribution zones can differ significantly for different plates, which affects their hydraulic resistance and the uniformity of flow distribution between the plates. According to the data [5–6], the proportion of the pressure drop in the inlet and outlet zones of some heat exchangers formed by the plates can reach 50% and more, especially at smaller β angles of the corrugation inclination to the vertical axis of the plate.

For mathematical simulation of thermal and hydraulic characteristics an interplate channel is considered to consist of a main corrugated field which effects significantly on heat transfer (Fig. 2).

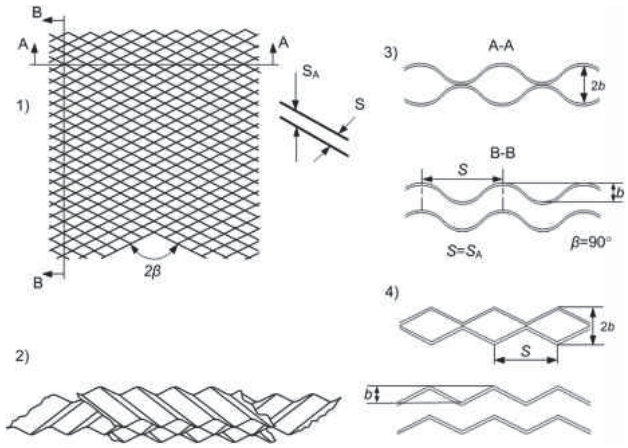

FIGURE 2. Various forms of corrugation of plate:
1, 2 – intersection of adjacent plates; 3 – cross-sections of channels for a sinusoidal shape; 4 – cross-sections of channels for triangular corrugations

The problem was solved in a 3-dimensional setting. Four options for shapes of heat transfer plates in a longitudinal section were considered (Fig. 3– 6). Boundary conditions were formulated, and, on their basis, coefficients of local resistances ζ and temperature efficiency *Et* for each model of the heat exchanger were calculated.

Model 1

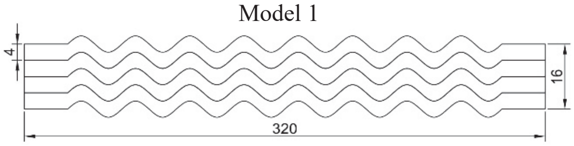

FIGURE 3. Model of heat exchanger with sinusoidal profile

Model 2

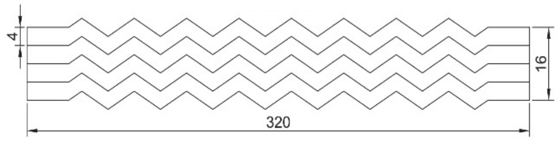

FIGURE 4. Model of heat exchanger with a triangular profile

Model 3

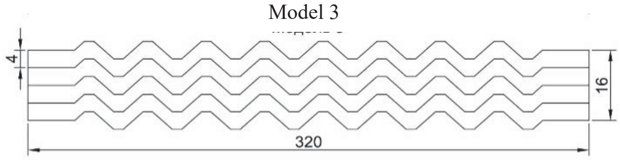

FIGURE 5. Model of heat exchanger with a trapezoidal profile

Model 4

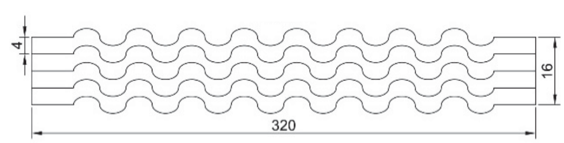

FIGURE 6. Model of exchanger with ellipsoidal profile

Thermal efficiency is calculated by the formula:

$$E_t = \frac{t_{\text{heated}} - t_{\text{cold}}}{t_{\text{hot}} - t_{\text{cold}}}, \tag{1}$$

where $t_{\text{heated}}, t_{\text{cold}}, t_{\text{hot}}$ are temperatures of heated, cold and hot water, °C.

Calculated total pressure losses in the channels are found, their values are averaged, the coefficient of local resistances of the apparatus according to the formula:

$$\zeta = \frac{\Delta P_n}{P_\partial}, \tag{2}$$

where ΔP_n is an averaged value of total pressure drop;

P_∂ is a dynamic pressure value, Pa;

$$P_\partial = \frac{\rho \cdot v^2}{2}, \tag{3}$$

ρ, v is density and speed at the inlet of the channels, m/s.

After creating and checking mesh quality criteria, when analyzing the model, the data on the obtained meshes are unloaded, where the number of boundary and internal elements and the total number of computational meshes are indicated. The data are presented in table 2–5.

TABLE 2. Data of obtained meshes of heat exchange plates with a sinusoidal profile

	Boundary	**Inner**
Nodes	445 042	5 042 608
Faces	230 208	8 251 045
Total number of computational meshes		1 704 005

TABLE 3. Data of obtained meshes of heat exchange plates with a trapezoidal profile

	Boundary	**Inner**
Nodes	367 985	3 823 101
Faces	199 196	6 489 312
Total number of computational meshes		1 396 459

TABLE 4. Data of obtained meshes of heat exchange plates with a triangular profile

	Boundary	**Inner**
Nodes	201 892	1 939 703
Faces	109 188	3 347 536
Total number of computational meshes		731 327

TABLE 5. Data of obtained meshes of heat exchange plates with a ellipsoidal profile

	Boundary	**Inner**
Nodes	421 401	2 789 810
Faces	138 757	4 692 060
Total number of computational meshes		994 975

Turning to the problem solution, it is necessary to introduce operational conditions: the temperature of the environment is 293 *K,* the atmospheric pressure is 101 325 *Pa,* the gravitational axis y, equal to the value of gravitational acceleration, is 9.81 m/s^2. Next, a modeling method is selected: whether an energy conservation equation calculation is indicated or should be made. In the work the equation of energy conservation is taken into account. In the numeric simulation the k-epsilon model of fluid flow was used [7]. Constant values taken for cold water are: the density ρ_0= 999.8 kg/m^3, the heat capacity c_p =4204 *J / (kg · K)*, the viscosity coefficient μ=1547·10^{-6}*Pa·c*, the coefficient of thermal conductivity λ=0.5715 *W / (m · K)*. Constant values taken for hot water are: the density ρ_0= 934.6 *kg/m*^{3}, the heat capacity c_p = 4266 *J / (kg · K)*, the viscosity coefficient μ=217.8·10^{-6}*Pa·c*, the coefficient of thermal conductivity λ=0.686 *W / (m · K)*.

The plate thickness is 1 mm, cold water is supplied through one half of the channels, hot water is supplied through the other. The length of the apparatus and channels is 320 mm, the width of each channel is 20 mm, the height is 4 mm; the roughness of the plate surface is taken as 1.25 μm; the outer walls of the channels are adiabatic; the inner walls have the coefficient of heat conductivity $\lambda = 202$ W / (m · K); the temperature at the inlet to the cold water channels is 278 *K* (5 °C), the temperature at the inlet to the hot water channels is 403 *K* (130 °C).

For the improved "treatment" of the walls the calculation is carried out with an additional function "enhanced wall treatment" [8–9]. Individual models are mixed in a two-layer approach using the damping function so that the transition between them becomes smoother.

To prevent backflow, which may occur in case if there is a lack of the inlet pressure, the backflow temperature is set [10–12]. Values of backflow temperature are taken on average as 350 K.

At the following stage, the conditions for convergence of all parameters are set, next the number of iterations is introduced which are necessary in the case if the program will not reach the convergence, the calculation will stop at the specified number of iterations.

To analyze the models, it is necessary to create a two-dimensional plane, on which necessary calculation results will be graphically displayed: values of temperature, speed, turbulence, pressure [13]. To create the plane, the coordinate of an initial point, and a normal according to which the plane will be constructed are set (Fig. 7–10).

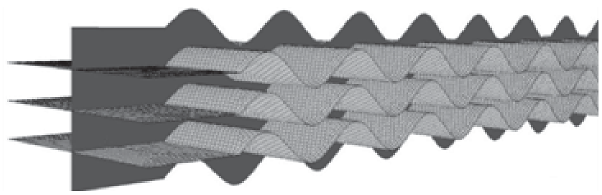

FIGURE 7. Plane for displaying graphic calculation results of model with a sinusoidal profile

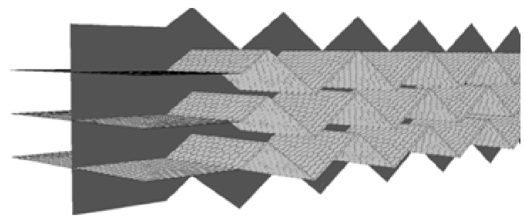

FIGURE 8. Plane for displaying graphic calculation results of model with a triangular profile

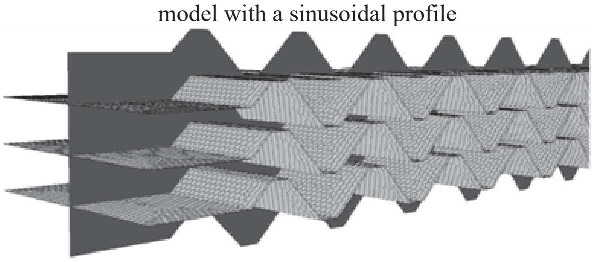

FIGURE 9. Plane for displaying graphic calculation results of model with a trapezoidal profile

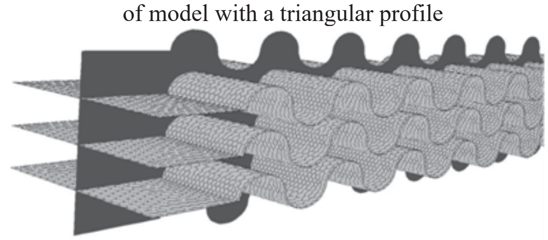

FIGURE 10. Plane for displaying graphic calculation results of model with an ellipsoidal profile

Next, the process is initialized, in which the program automatically sets a random value followed by the calculation. If an error was made at this stage of creating a model, computational mesh, model description and designation of boundary conditions, the calculation does not lead to a constant value [14–15]. Therefore, the correct mesh dimension is an important condition.

CALCULATION AND ANALYSIS OF OBTAINED DATA

The fluid flow is considered in a laminar region at Re < 400 and a transition region at 400 < Re < 1000. The internal flow of the plate heat exchanger can be considered as a fully developed turbulent one at Re > 1000. Particularly, the k-epsilon model is known as a suitable model for flows that involve the curvature of current and vortices. Therefore, speeds are taken such that the Re number is within the given boundaries.

It is possible to observe the alternation of flow direction by the speed profiles. The speed values are indicated on the color palette, where a blue color corresponds to a minimum speed, while a red color corresponds to a maximum speed. From these visual data we can suggest where stagnant zones will be formed, in which the chance of scale and stone formation is great.

Due to the turbulent zones, we can judge where the flow will self-purify from precipitated salts, as well as observe how the layers of the flow are mixing for better heat transfer. However, it is worth noting that the higher is the degree of intensification, the higher will be the final values of pressure losses in the channel.

All these data should be considered and analyzed for both cold water and hot water flows since the higher is the temperature, the easier salts precipitate and scale is formed, and, correspondingly, better chemical water treatment is required, which is not always feasible.

The speed and turbulence profiles of the flow at speeds of 0.01 m / s, 0.2 m / s, 0.5 m / s for the model with a sinusoidal profile are shown in Fig. 11–13.

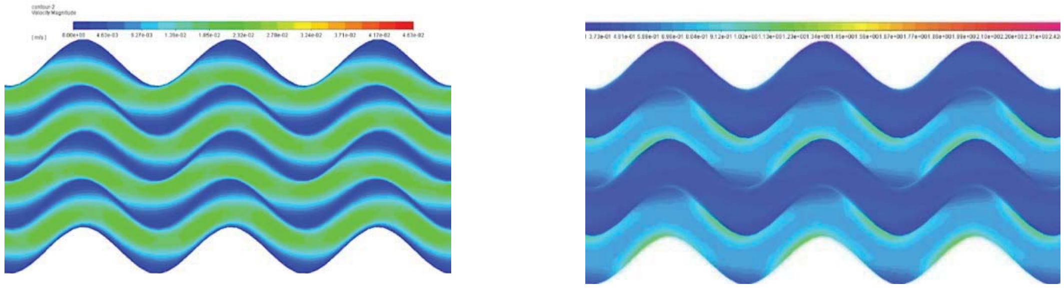

FIGURE 11. Profile of speed and turbulence for model with a sinusoidal profile at v=0.01 m/s, Re=43

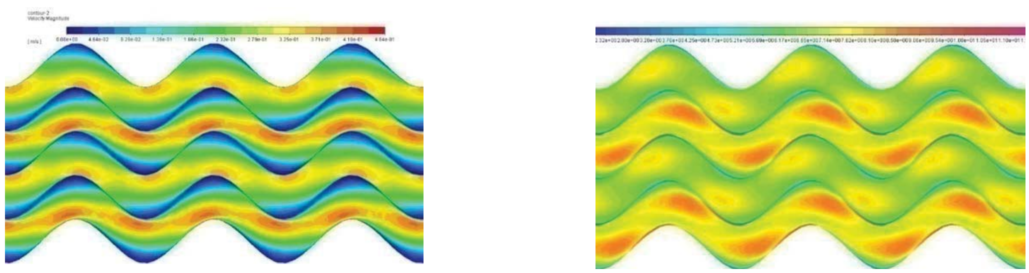

FIGURE 12. Profile of speed and turbulence for model with a sinusoidal profile at v=0.2 m/s, Re=866

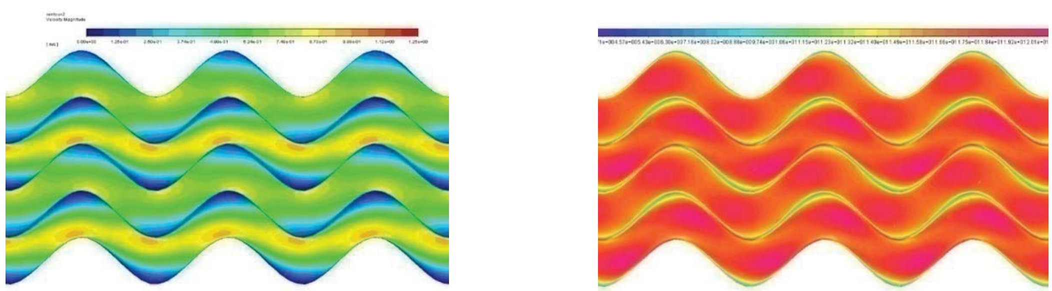

FIGURE 13. Profile of speed and turbulence for model with a sinusoidal profile at v=0.5 m/s, Re=2165

These pictures show that the main flow covers practically the entire area of the channel, and the stagnant zones where the speed value tends to zero are located mainly in the upper and lower crests of the waves relative to the flow. At the same time, the turbulence value at these sites is not quite equal to zero, consequently, salts are likely to be thrown out from the stagnant zones into the main flow. These images show that, while the speed increases, the main flow narrows and tries to stretch in a straight line along the way of the least resistance. At the same time, the size of the stagnant zones increases. The turbulent zones lie outside the central flow, which indicates its lower ability to mix. Also, it is worth noting that, judging by the color scheme, the turbulent zones are mainly formed before all flexions, but immediately after them there is no turbulence, which, together with the low value of the main flow speed, results in salt deposition.

At a speed of 0.5 m/s all stagnant and turbulent zones become most obvious. The turbulent zones are fewer at the side of the hot flow, and the speed profile is more “blurred”. When comparing the speed profile with the turbulence profile, one can notice that the turbulent zones intersect in some places with the central flow, which produces its partial mixing.

Based on the results, we can conclude that, with such a configuration of channels, a developed turbulent flow begins at the number Re ≈ 800. An entire turbulent flow is reached at higher speeds, as it is presented at Re more than 1300. At the same time, it is worth noting that, at similar speeds, and, accordingly, with the similar Re numbers, in this section the flow becomes turbulent more rapidly and the turbulence is more even alongside the channel.

Comparing the “graphs” of the speed and turbulence, one can see that in this case the zones of turbulence partially cover the main flow.

The results of all the calculations made are presented in table 6.

TABLE 6. Results of calculations made

Model with a triangular profile	v, m/s	0.01	0.05	0.10	0.20	0.30	0.50
	t_{out}, K	346.68	346.61	335.71	322.59	315.58	308.00
	efficiency	54.94	54.89	46.16	35.67	30.07	24.00
	P before, Pa	10.33	111.66	377.01	1384.25	3043.98	8440.00
	P after, Pa	0.32	1.57	5.78	22.36	49.27	133.83
	dP, Pa	10.01	110.09	371.23	1361.89	2994.71	8306.18
	P_{dyn}, Pa	0.05	1.25	5.00	20.00	44.99	124.98
	KMC	200.30	88.09	74.26	68.11	66.56	66.46
Model with a sinusoidal profile	v, m/s	0.01	0.05	0.10	0.20	0.30	0.50
	t_{out}, K	346.19	348.97	340.23	328.73	320.94	312.25
	efficiency	54.55	56.78	49.79	40.59	34.35	27.40
	P before, Pa	11.49	111.52	347.31	1124.15	2241.00	5326.10
	P after, Pa	0.30	1.58	5.83	22.52	49.78	135.48
	dP, Pa	11.18	109.94	341.48	1101.63	2191.22	5190.62
	P_{dyn}, Pa	0.05	1.25	5.00	20.00	44.99	124.98
	KMC	223.74	87.97	68.31	55.09	48.70	41.53
Model with trapezoidal profile	v, m/s	0.01	0.05	0.10	0.20	0.30	0.50
	t_{out}, K	347.99	348.90	339.78	327.91	320.45	311.90
	efficiency	55.99	56.72	49.42	39.93	33.96	27.12
	P before, Pa	12.80	128.18	402.76	1340.10	2784.12	7106.62
	P after, Pa	0.30	1.58	5.83	22.50	49.68	134.76
	dP, Pa	12.49	126.60	396.93	1317.60	2734.45	6971.85
	P_{dyn}, Pa	0.05	1.25	5.00	20.00	44.99	124.98
	KMC	249.88	101.30	79.40	65.89	60.78	55.79
Model with ellipsoidal profile	v, m/s	0.01	0.05	0.10	0.20	0.30	0.50
	t_{out}, K	348.76	350.01	340.23	327.47	320.33	312.28
	efficiency	56.61	57.61	49.78	39.58	33.86	27.42
	P before, Pa	18.42	193.93	616.63	2025.80	4091.52	9957.88
	P after, Pa	0.33	1.57	5.77	22.14	48.86	133.21
	dP, Pa	18.09	192.36	610.86	2003.67	4042.66	9824.68
	P_{dyn}, Pa	0.05	1.25	5.00	20.00	44.99	124.98
	KMC	361.95	153.92	122.20	100.20	89.85	78.61

Based on the obtained data, the graph of dependence of the efficiency of the heat exchanger on the speed flow (Fig. 14), and the graph of dependence of the total pressure on the speed flow (Fig. 15) were constructed.

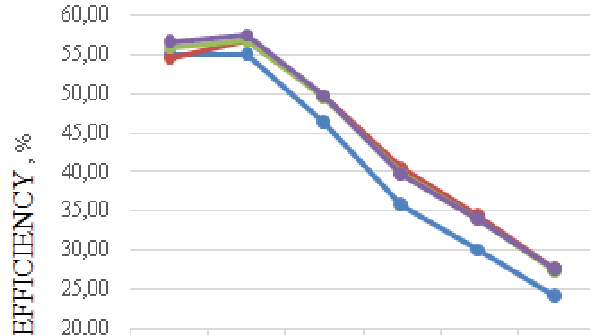

	0,01	0,05	0,10	0,20	0,30	0,50
tr	54,94	54,89	46,16	35,67	30,07	24,00
sinus	54,55	56,78	49,79	40,59	34,35	27,40
trap	55,99	56,72	49,42	39,93	33,96	27,12
ellips	56,61	57,61	49,78	39,58	33,86	27,42

speed, m/s

FIGURE 14. Graph of dependence of efficiency on flow speed

By this graph we can conclude that for the selected models the most efficient speed is 0.05 m/s where the highest heat transfer is achieved. A further increase in the flow rate leads to a decrease in this indicator. Also, among the models presented, the least useful properties are observed in the plates with a triangular profile, while the rest of the models are approximately equal to each other. For a more accurate analysis, the values of each model are duplicated in table 6.

It is worth noting that in the model with ellipsoid plates the efficiency at starting speeds is higher than in the other models. This is associated with the fact that, due to this shape of the plates, the main flow which tries to follow the path of minor resistance is forced into the zones of turbulence which, in addition, begins to form even earlier, due to this, is mixed, and participates better in the heat exchange process. However, with the increasing speed, this advantage disappears.

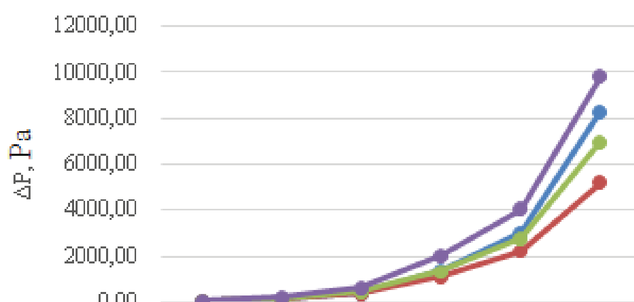

	0,01	0,05	0,10	0,20	0,30	0,50
tr	10,01	110,09	371,23	1361,8	2994,7	8306,1
sinus	11,18	109,94	341,48	1101,6	2191,2	5190,6
trap	12,49	126,60	396,93	1317,6	2734,4	6971,8
ellips	18,09	192,36	610,86	2003,6	4042,6	9824,6

speed, m/s

FIGURE 15. Graph of dependence of total pressure losses on flow speed

CONCLUSION

Numeric simulation of the heat transfer process in the plate heat exchanger in a longitudinal section was carried out using the ANSYS software package. Four options of plates were considered: those with sinusoidal, triangular, trapezoidal, and ellipsoidal profiles.

Based on the obtained simulation results, namely, the speed profile, turbulence, obtained values of pressure losses and temperatures, as well as the graphs constructed according them, we can conclude that, when considering a longitudinal section with an increasing speed, the shape of the corrugated plate impact on the heat transfer characteristics to a lesser extent, and impact on the hydraulic losses to a more extent.

It is worth noting that water flows in the cold channels, having a high viscosity, always try to move on in one beam and along the path of the least resistance, while the specific features of motion in the channels of the hot heat carrier vary depending on the model.

Of the four models under consideration, at relatively low speeds, the most successful model is that with the plates forming an ellipsoidal profile, and, with a further increase in speed, that with a sinusoidal profile, since it is in them that the optimal ratio of efficiency to pressure losses is achieved.

From the research results it is obvious that the intense turbulence of the flow grows only at relatively low speeds, and does not mean the improved thermal characteristics at higher speeds, since in the model with an ellipsoidal profile the highest pressure losses and turbulence are observed with the lack of the growth of the heat amount transferred through the plates. Also, this model has the largest number of “stagnant” zones which contribute to the appearance of deposits.

To improve streamlining and to decrease hydraulic losses in the design of plates, it is necessary to consider how the speed and turbulence profiles will look at operating speeds. Based on these data, it will be possible to modernize the curvature of plates so that they match better the flow style of hot and cold media.

REFERENCES

1. V. N. Baranovsky, L. M. Kovalenko, A. P. Yastrebenetsky, *Plate heat exchangers* (Mechanical Engineering, Moscow, 1973), p. 678.
2. O. G. Martynenko, A. A. Mikhalevicha, and V. K. Shikova, *Heat exchanger handbook (*Energy Atom Publishing, Moscow, 1987).
3. L. L. Tovazhnyansky, P. A. Kapustenko, and V. A. Tsibulnich, *Heat transfer and hydraulic resistance in the channels of plate heat exchangers* (Power Engineering, 1980).
4. GOST (State Standard) 25449-82 Heat exchangers water-to-water and steam-to-water. Types, basic parameters and dimensions (with Change No. 1)
5. P. Pongsoi, S. Pikulkajorn, and S. Wongwises, Int. J. Heat Mass Transfer (2016).
6. K. Lindqvis, Z. T. Wilson, E. Naess, and N. V. Sahinidis, *A machine learning approach to correlation development applied to fin-tube bundle heat exchanger* (Energies, 2018).
7. X. Q. Liu, J. L. Yu, and G. Yan, *Int. J. Heat Mass Transfer* (2016).
8. J. Kosprdova, “The Development of Centrifugal Turbo Compressor Stage Using CF”, in *The 20th International Conference on Hydraulics and Pneumatics*, Prague, September 29 – October 1, 2008, edited by Jindra Kosprdova, Jiri Oldrich (2008).
9. R. Puzyrewski *at al.,* Projekt KNB 8T10B00419, Etap 5 (Kwiecien, Gdansk, 2000).
10. J. M. Sorokes, *Side Stream Optimization Through the Use of Computational Fluid Dynamics and Model Testing Turbomachinery Sympos*, edited by J. M. Sorokes, D. A. Nye, N. D'Orsi, and R. Broberg (A&M, Texas, 2000).
11. J. Klemes, F. Friedler, I. Bulatov, and P. Varbanov *Sustainability in the process industry. Integration and optimization* (The McGraw-Hill Co-s. Inc, New York, USA, 2010).
12. P. S. Varbanov, Z. Fodor, J. J. Klemes, *Total site targeting with process specific minimum temperature difference* (DTmin, Energy, 2012).
13. R. K. Shah, D. P. Sekulic, *Fundamentals of heat exchanger design* (Wiley and Sons, New York, 2003).
14. D. Dovic, B. Palm, and S. Svaic, International Journal of Heat and Mass Transfer **52(19)** 4553–4563 (2009).
15. S. D. Pandey, and V. K. Nema, Energy **36(5)** 2997–3001 (2011).